

Elucidation of the biosynthesis of the methane catalyst coenzyme F₄₃₀

Simon J. Moore¹, Sven T. Sowa², Christopher Schuchardt², Evelyne Deery¹, Andrew D. Lawrence¹, José Vazquez Ramos², Susan Billig³, Claudia Birkemeyer³, Peter T. Chivers⁴, Mark J. Howard¹, Stephen E. J. Rigby⁵, Gunhild Layer² & Martin J. Warren¹

Methane biogenesis in methanogens is mediated by methyl-coenzyme M reductase, an enzyme that is also responsible for the utilization of methane through anaerobic methane oxidation. The enzyme uses an ancillary factor called coenzyme F₄₃₀, a nickel-containing modified tetrapyrrole that promotes catalysis through a methyl radical/Ni(II)-thiolate intermediate. However, it is unclear how coenzyme F₄₃₀ is synthesized from the common primogenitor uroporphyrinogen III, incorporating 11 steric centres into the macrocycle, although the pathway must involve chelation, amidation, macrocyclic ring reduction, lactamization and carbocyclic ring formation. Here we identify the proteins that catalyse the biosynthesis of coenzyme F₄₃₀ from sirohydrochlorin, termed CfbA–CfbE, and demonstrate their activity. The research completes our understanding of how the repertoire of tetrapyrrole-based pigments are constructed, permitting the development of recombinant systems to use these metalloprosthetic groups more widely.

Coenzyme F₄₃₀ is a modified tetrapyrrole that is required by methyl-coenzyme M reductase, the terminal enzyme in the process of methanogenesis^{1,2} (Fig. 1). This cofactor is responsible for the generation of about one billion tons of methane gas per annum, roughly one-third of which escapes into the atmosphere where it is photochemically converted into CO₂ (ref. 2), thus contributing to the greenhouse effect and global warming. More recently, methyl-coenzyme M reductase has also been implicated in the process of reverse methanogenesis (anaerobic methane oxidation)^{3–6}, which is mediated by bacterial/archaeal mats on the ocean floor. Methyl-coenzyme M reductase is an enzyme ensemble consisting of a dimer of heterotrimers (α₂β₂γ₂), catalysing the reversible reduction of methyl-coenzyme M (CH₃-S-CoM) and coenzyme B (HS-CoB) into the heterodisulfide CoM-S-S-CoB and methane⁷. Central to the mechanism of this powerful redox catalyst^{8,9} is the nickel porphinoide, coenzyme F₄₃₀ (–650 mV Ni^{+/2+} redox couple). Despite the indispensable role of coenzyme F₄₃₀ in the process of methanogenesis and carbon cycling, the assembly of this unique cofactor had not been determined¹⁰.

As a modified tetrapyrrole, the synthesis of coenzyme F₄₃₀ is based on the macrocyclic template of uroporphyrinogen III (refs 11, 12, 13), from which all haems, chlorophylls, sirohemes, corrins, bilins and haem d₁ are derived. However, coenzyme F₄₃₀ differs from these other modified tetrapyrroles in the nature of the centrally chelated metal ion and in the oxidation state of the macrocycle, a tetrahydroporphyrinogen, the most reduced member of the family¹³. As well as the four pyrrole-derived rings found in all modified tetrapyrroles (labelled A–D; Fig. 1a), coenzyme F₄₃₀ also contains two extra rings (E and F; Fig. 1a). Ring E is a lactam derived from the amidated acetic acid side chain attached to ring B, while the keto-containing ring F originates from the propionic acid side chain on ring D. Radiolabelling experiments indicated that the biosynthesis of coenzyme F₄₃₀ proceeds via sirohydrochlorin, the metal-free precursor of siroheme¹⁴. Moreover, under depleted nickel growth conditions, *Methanothermobacter marburgensis* was found to accumulate a 15,17³-*seco* intermediate (*seco*-F₄₃₀) missing ring F (ref. 15). This intermediate could be converted into coenzyme F₄₃₀ by cell-free extracts in the presence of ATP¹⁵, indicating that this

seco-F₄₃₀ may represent the penultimate intermediate in the biosynthetic pathway.

Potential gene clusters

With the knowledge that the biosynthesis of coenzyme F₄₃₀ has to involve metal ion chelation, side-chain amidation and macrocyclic ring reduction, we sought the clustering of corresponding potential genes for coenzyme F₄₃₀ biosynthesis (given the acronym *cbf*) within the genomes of a range of methanogens. Notably, this approach allowed us to identify such a grouping in several methanogens, including *Methanosarcina barkeri*, *Methanomassiliicoccus intestinalis* and *Methanocella conradii*, as shown in Fig. 1b. These clusters all contain genes for a small type II chelatase¹⁶ (CfbA), followed by a MurF-like ligase¹⁷ (CfbB) and orthologues of the NifD and NifH components of nitrogenase (CfbC and CfbD, respectively). The latter are also orthologues of BchN and BchL, catalytic components of the tetrapyrrole-reducing dark-operative protochlorophyllide reductase (DPOR)¹⁸ enzyme that is involved in bacteriochlorophyll synthesis. The last gene of the cluster encodes an (CfbE) that is similar to the CobB/CbiA *a,c*-diamide synthetase enzymes found in cobalamin biosynthesis¹⁹. In addition, *M. intestinalis* contains the genes for the transformation of glutamic acid into precorrin-2, the direct precursor of sirohydrochlorin, within the same gene cluster. The *cbf* genes from *M. barkeri* were amplified and cloned to allow for the characterization of the encoded products (Extended Data Table 1).

Nickel chelatase CfbA

We previously showed that CfbA (Mbar_A0344) can act as a cobalto-chelatase, and named it CbiX^S (ref. 16). Here, using a higher concentration of Ni²⁺ in the assays (50 μM rather than 20 μM), the conversion of sirohydrochlorin to Ni²⁺-sirohydrochlorin by CfbA could be followed by ultraviolet/visible (UV/Vis) absorption spectroscopy (Extended Data Fig. 1), demonstrating that CfbA is able to catalyse the insertion of nickel as well as cobalt into sirohydrochlorin *in vitro*. The specific activity of CfbA for Ni²⁺ insertion *in vitro* was determined as 3.4 ± 0.5 nmol min⁻¹ mg⁻¹, which is considerably lower than that observed for Co²⁺ insertion (122 nmol min⁻¹ mg⁻¹)¹⁶. The assays were performed with

¹School of Bioscience, University of Kent, Giles Lane, Canterbury, Kent CT2 7NJ, UK. ²Institute of Biochemistry, Leipzig University, 04103 Leipzig, Germany. ³Institute of Analytical Chemistry, Leipzig University, 04103 Leipzig, Germany. ⁴Department of Chemistry, School of Biological and Biomedical Sciences, Durham University, Durham DH1 3LE, UK. ⁵Manchester Institute of Biotechnology, School of Chemistry, University of Manchester, 131 Princess Street, Manchester M1 7DN, UK.

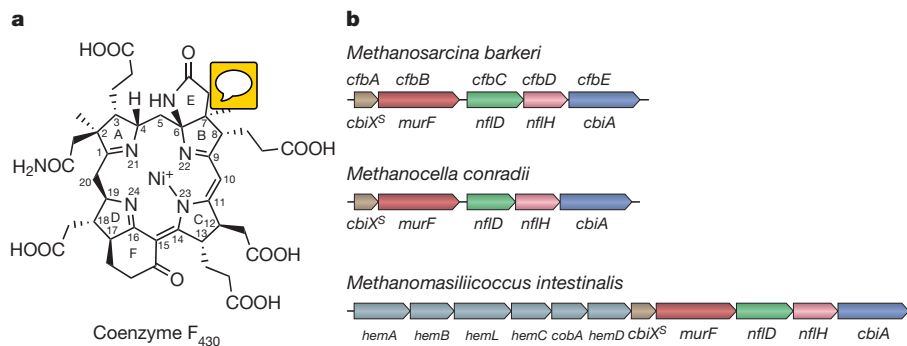


Figure 1 | Coenzyme F₄₃₀ and biosynthesis gene clusters in methanogens. **a**, Coenzyme F₄₃₀ structure showing the numbering of the pyrrole rings A–D, lactam ring E and cyclohexanone ring F, and the C and N atoms. **b**, Coenzyme F₄₃₀ biosynthesis (*cfb*) gene clusters identified in this study. Homologous genes are shown in the same colour. Gene designations below the arrows represent the original annotation. The

reagents that were originally devised for cobalt insertion and therefore optimization is required through the use of different buffers and pH values to determine conditions that may allow for enhanced Ni²⁺ insertion. Hence, the *in vivo* activity of the chelatase enzyme might be much faster than that observed *in vitro*.

To this end, the activity of CfbA as a nickel-chelatase was also probed *in vivo*. Under aerobic conditions, *Escherichia coli* does not import nickel, although anaerobically a high-affinity multicomponent system, *nikA–nikE*, is activated^{20–22}. We attempted to produce Ni²⁺-sirohydrochlorin in *E. coli* by linking the expression of the genes for the production of precorrin-2 (*cobA*) and sirohydrochlorin (*sirC*) with the nickel chelatase (*cfbA*, also known as *cbiX_s*) by cloning them consecutively on the same plasmid to give pETcoco-2-cobA-sirC-cfbA. Additionally, to maximize the availability of Ni²⁺ for CfbA, we added the gene for the *Helicobacter pylori* nickel transporter (*nixA*)²³ to the construct to give pETcoco-2-cobA-sirC-cfbA-nixA. *E. coli* cells containing pETcoco-2-cobA-sirC-cfbA grown in the presence of nickel, at concentrations between 25 μM and 100 μM, were dark brown in colour. However, *E. coli* containing pETcoco-2-cobA-sirC-cfbA-nixA grown under the same conditions were observed to have a dark violet pigmentation (Extended Data Fig. 1). The violet pigment was identified as Ni²⁺-sirohydrochlorin by mass spectrometry (Extended Data Fig. 2). Altogether, these results show that CfbA can act as a nickel-chelatase both *in vitro* and *in vivo*. Given the large accumulation of Ni²⁺-sirohydrochlorin within the recombinant *E. coli*, several milligrams per litre of culture, and the lack of free sirohydrochlorin, we can state that CfbA is more than active enough *in vivo* to support F₄₃₀ synthesis. The discrimination between metals such as Ni²⁺ and Co²⁺ *in vivo* by the chelatase must reflect the different availabilities of these divalent metal ions in the bacterial cytoplasm²⁴.

Amidase CfbE

To investigate the *in vivo* activity of the putative *a,c*-diamide synthetase (amidotransferase or amidase), CfbE (Mbar_A0348), we co-transformed *E. coli* with the CfbE-producing plasmid pET14b-cfbE and with pETcoco-2-cobA-sirC-cfbA-nixA. The resulting strain was grown in the presence of exogenous nickel and was harvested as a dark violet pellet. Extraction of the His₆-tagged CfbE by immobilized metal affinity chromatography (IMAC) from the lysed cell pellet resulted in the co-isolation of a tightly bound violet-coloured pigment (Extended Data Fig. 2), in line with the observation that many tetrapyrrole biosynthetic enzymes bind their products tightly to facilitate direct metabolite channelling²⁵. Analysis of this pigment by high-performance liquid chromatography tandem mass spectrometry (HPLC–MS) revealed that it elutes as a single peak at 20.5 min with a mass of 917 Da, consistent with the expected molecular mass for Ni²⁺-sirohydrochlorin diamide (C₄₂H₄₆N₆O₁₄Ni). In comparison, a standard of Ni²⁺-sirohydrochlorin

genes are: *M. barkeri*: *cfbA* (Mbar_A0344), *cfbB* (Mbar_A0345), *cfbC* (Mbar_A0346), *cfbD* (Mbar_A0347), *cfbE* (Mbar_A0348); *M. conradii*: *cfbA* (MTC_0061), *cfbB* (MTC_0062), *cfbC* (MTC_0063), *cfbD* (MTC_0064), *cfbE* (MTC_0065); *M. intestinalis*: *cfbA* (H729_08045), *cfbB* (H729_08040), *cfbC* (H729_08035), *cfbD* (H729_08030), *cfbE* (H729_08025).

(C₄₂H₄₄N₄O₁₆Ni) eluted on HPLC–MS as a triple peak between 23 and 25 min, with the predominant species showing a mass of 919 Da (Extended Data Fig. 2).

The amidase activity of CfbE was investigated by incubating purified enzyme with Ni²⁺-sirohydrochlorin, MgATP and glutamine. HPLC–MS analysis of the reaction products showed a single peak at 20.5 min, with a mass of 917 Da (Extended Data Fig. 2). By replacing glutamine with ¹⁵NH₃ in the CfbE reaction, it was found that the main product peak eluted at the same retention time, but exhibited an increased mass of two units to 919 Da, consistent with the incorporation of the heavy isotope into the tetrapyrrole side chains during the reaction (Extended Data Fig. 2). NMR analysis of Ni²⁺-sirohydrochlorin *a,c*-diamide after labelling of the side chains with ¹⁵NH₃ confirmed the incorporation of the two amide groups into the acetic acid side chains attached to rings A and B (Extended Data Figs 2 and 3; Supplementary Table 1).

Single turnover reactions demonstrated that the order of side-chain amidation was random, whereas time course studies indicated a direct conversion of the substrate into the diamide product, without release of the monoamide. Sirohydrochlorin also acted as a substrate for CfbE but only produced a monoamide species in a much slower reaction, highlighting that Ni²⁺-sirohydrochlorin is the preferred substrate for the amidotransferase.

Finally, kinetic parameters were determined for the amidation reaction from a study of both the ATPase and glutaminase activities of CfbE in the presence of Ni²⁺-sirohydrochlorin (Extended Data Fig. 4). With glutamine as the variable substrate and ATP fixed at 0.5 mM, the Michaelis constant (*K_m*) and turnover number were estimated to be 46 μM and 0.78 min⁻¹, respectively. When the concentration of ATP was varied, with glutamine fixed at 1 mM, the *K_m* value and turnover number were estimated to be 28 μM and 1.03 min⁻¹, respectively. Furthermore, the enzyme was found to be inactive with other metallo-sirohydrochlorins such as siroheme and Co²⁺-sirohydrochlorin.

Reductase CfbC/CfbD

The CfbC and CfbD proteins (Mbar_A0346, Mbar_A0347) belong to the family of the so-called class IV nitrogenase NflD/H^{26,27} that was shown to lack nitrogenase activity in *Methanocaldococcus jannaschii* but was suspected of being involved in a methanogen-specific process¹⁸. Recombinant CfbC and CfbD were produced as His₆-tagged proteins in *E. coli* and purified under anaerobic conditions, but UV/Vis absorption spectra and iron and sulfide determination assays indicated that Fe–S cluster incorporation was very low (<0.5 mol of iron and about 1 mol of sulfide per mol of protein). These values were improved through chemical Fe–S cluster reconstitution. The resulting iron and sulfide contents suggested the presence of inter-subunit [4Fe–4S] clusters. Consistent with this, both CfbC and CfbD migrated as dimers during gel filtration chromatography, although CfbD migrated as a monomer in the absence

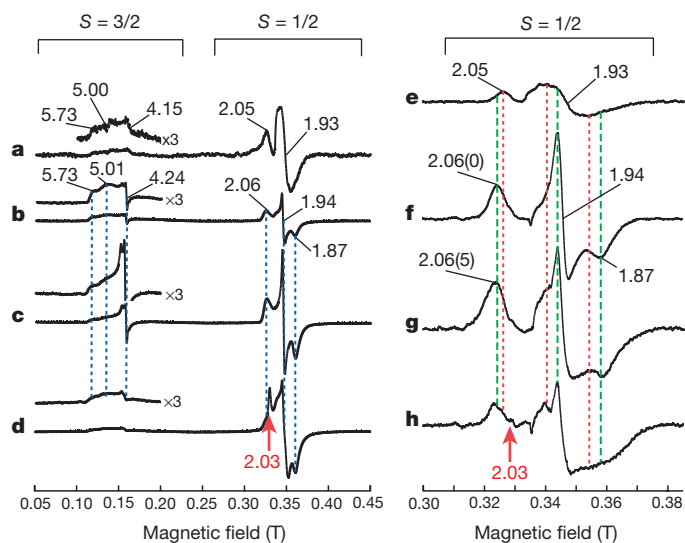


Figure 2 | EPR characterization of CfbC and CfbD. **a–d**, X-band continuous wave EPR spectra of dithionite-reduced proteins: CfbC (**a**), CfbD (**b**), CfbD plus excess MgADP (**c**), CfbD plus excess MgATP (**d**). In **b–d**, the same vertical scale, protein concentration and dithionite concentration are used. **e–h**, EPR spectra of CfbC (**e**), CfbD (**f**), 1:1 mixture of CfbC and CfbD (**g**), 1:1 mixture of CfbC and CfbD plus excess MgATP (**h**). The same vertical scale, protein concentration and dithionite concentration are used for **e–h**. Experimental parameters: microwave power 0.5 mW, field modulation amplitude 0.7 mT, temperature 15 K.

of the cluster. The presence of [4Fe-4S] centres on dithionite-reduced CfbC/CfbD was confirmed by electron paramagnetic resonance (EPR) spectroscopy, in which features in the $g = 4$ and $g = 2$ regions arise from the $S = 3/2$ and $S = 1/2$ spin states of [4Fe-4S] $^{1+}$ clusters present in both proteins (Fig. 2). Although CfbC is insensitive to the presence of MgATP, CfbD shows both MgADP and MgATP-dependent changes in the $S = 1/2$ and $S = 3/2$ signals (Fig. 2b–d). In mixtures of CfbC and CfbD, the $S = 1/2$ signal for CfbD is much more intense than that of CfbC at the same protein concentration (Fig. 2g), suggesting that CfbC has the lower midpoint redox potential (E_M) and hence the need for ATP-coupled ‘uphill’ electron transfer. The addition of MgATP to the protein mixtures produces the spectrum of Fig. 2h, showing a greater reduction of CfbC and less reduced CfbD in keeping with the proposed MgATP-dependent electron transfer from CfbD to CfbC.

The reductase activity was investigated by incubating reconstituted CfbC/CfbD with Ni^{2+} -sirohydrochlorin *a,c*-diamide, MgATP and sodium dithionite as the source of electrons. During the incubation, the characteristic UV/Vis absorbance of Ni^{2+} -sirohydrochlorin *a,c*-diamide at 594 nm decreased, and new absorption features around 446 and 423 nm appeared (Fig. 3). Interestingly, the decrease in absorbance at 594 nm and the concomitant increase in absorbance at 446 nm were observed only during the first 1.5 h of incubation, and the absorption feature at 446 nm shifted to 423 nm during prolonged incubation for 14–22 h without any further signal decrease at 594 nm. When CfbC or MgATP were omitted from the assay as a control, the UV/Vis absorption spectrum did not change (Fig. 3).

HPLC analysis of the tetrapyrrole content of the CfbC/CfbD assay mixture after 1.5 and 22 h of incubation revealed that the respective reaction products eluted at the same retention time but exhibited clearly different UV/Vis absorption spectra (Fig. 3). Whereas the product that formed after 1.5 h exhibited absorption features at 309, 358 and 446 nm, which is very similar to the spectrum of a synthetic Ni^{2+} -tetrahydrocorphinat 28 , the product formed after 22 h showed absorption at 305 and 428 nm, notably similar to the absorption spectrum of *seco*-F $_{430}$ (ref. 15). Both reaction products exhibited a mass of 923 Da, consistent with the theoretical mass of Ni^{2+} -hexahydrochlorin *a,c*-diamide or *seco*-F $_{430}$ (Extended

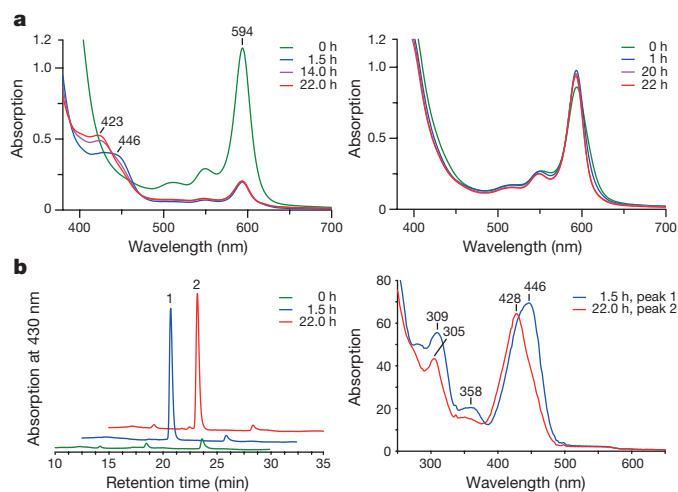


Figure 3 | Enzymatic activity of CfbC and CfbD. **a**, Left, UV/Vis absorption spectra of the conversion of Ni^{2+} -sirohydrochlorin *a,c*-diamide (green line) to Ni^{2+} -hexahydrochlorin *a,c*-diamide (blue line), catalysed by CfbC and CfbD during 1.5 h and autocatalytic formation of the lactam ring E yielding *seco*-F $_{430}$ (pink and red lines) during 14–22 h of incubation. Right, UV/Vis absorption spectra of the control reaction lacking CfbC. **b**, HPLC analysis (left) of the reaction products from **a** after 1.5 and 22 h of incubation with diode-array detection (right). Characteristic absorption features of the reaction products are indicated.

Data Fig. 5). Together, these results suggest that during the first part of the reaction (1.5 h) CfbC/CfbD reduces the macrocycle through the addition of 6 electrons and 7 protons. The subsequent reaction (22 h), which may be spontaneous 15,29,30 , represents lactam formation on ring E and the generation of *seco*-F $_{430}$. Indeed, the structure of the *seco*-F $_{430}$ intermediate was confirmed using 2D heteronuclear NMR spectroscopy in D $_2$ O (Extended Data Fig. 6, Supplementary Table 2). The overall effect of the reduction process and ring lactamization is to introduce 7 new steric centres into the macrocycle, indicating that the CfbC/CfbD catalyses a highly orchestrated spatial and regio-selective reaction.

It is interesting to note that nitrogenase and nitrogenase-like proteins catalyse difficult reduction reactions, or at least reactions that require a low redox potential, including the reduction of N_2 to NH_3 (ref. 31), protochlorophyllide to chlorophyllide 26 , and Ni^{2+} -sirohydrochlorin diamide to Ni^{2+} -hexahydrochlorin diamide. Clearly, the role of CfbC/CfbD more closely parallels the stereospecific reduction of the C17–C18 double bond catalysed by the orthologous DPOR during chlorophyll and bacteriochlorophyll biosynthesis 26 , but the requirement in F $_{430}$ biosynthesis for only the NifD and NifH homologues suggests that this system may provide a simpler model for the coupling of ATP hydrolysis to such biological reduction processes. Notably, we have yet to identify the source of the electrons, such as a ferredoxin, for the saturation of

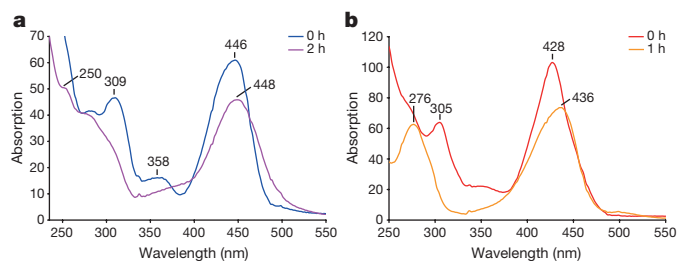


Figure 4 | Enzymatic activity of CfbB. **a**, UV/Vis absorption spectra (after HPLC separation) of the substrate Ni^{2+} -hexahydrochlorin *a,c*-diamide (blue line) and the reaction product observed after incubation with CfbB and ATP for 2 h (pink line). **b**, UV/Vis absorption spectra (after HPLC separation) of the substrate *seco*-F $_{430}$ (red line) and the reaction product observed after incubation with CfbB and ATP for 1 h (orange line).

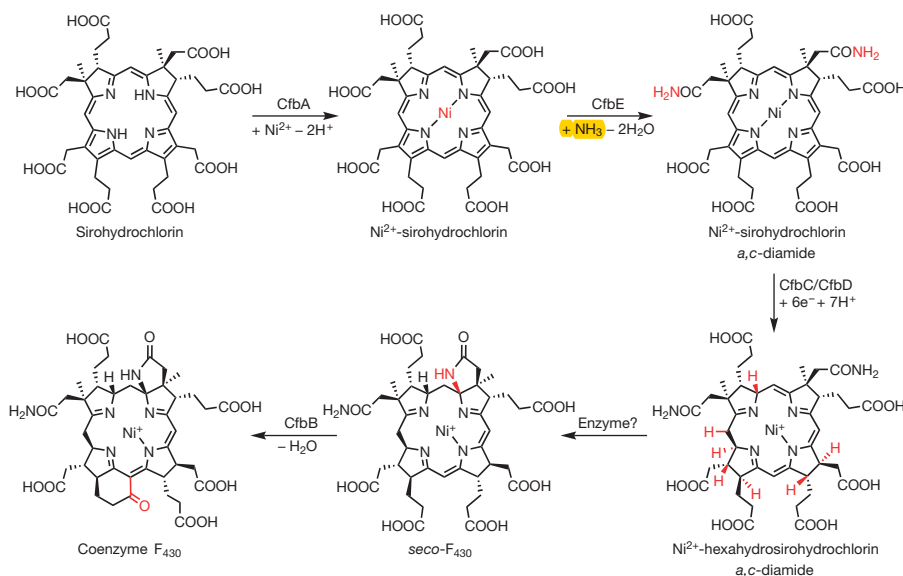


Figure 5 | Biosynthesis of coenzyme F₄₃₀ from sirohydrochlorin.

The overall series of reactions required for the transformation of sirohydrochlorin into coenzyme F₄₃₀. There are four enzymatic steps, requiring CfbA, CfbE, CfbC/CfbD and CfbB, as well as one spontaneous

the three double bonds during F₄₃₀ biosynthesis, an omission that may hinder the heterologous production of the coenzyme in *E. coli*.

seco to F₄₃₀ by CfbB

To investigate the function of recombinant, purified CfbB (Mbar_A0345), the protein was added to an assay mixture containing either Ni²⁺-hexahydrosirohydrochlorin *a,c*-diamide formed by the action of CfbC/CfbD or *seco*-F₄₃₀ together with MgATP. At different time points, the tetrapyrrole content of the mixtures was analysed by HPLC with diode-array detection and HPLC–MS. As shown in Fig. 4, CfbB converted both substrates into reaction products as indicated by the changes of the characteristic UV/Vis absorption spectra. For the mixture containing the Ni²⁺-hexahydrosirohydrochlorin *a,c*-diamide, the major absorption peak at 446 nm slightly shifted to 448 nm and the features at 309 and 358 nm disappeared. For the reaction mixture containing *seco*-F₄₃₀, the newly formed product exhibited absorption features identical to those of authentic coenzyme F₄₃₀ with maxima at 276 and 436 nm (Fig. 3 and Extended Data Fig. 7). For both reaction products, HPLC–MS revealed a mass of 905 Da, consistent with the theoretical mass of coenzyme F₄₃₀ (Extended Data Fig. 7). Considering the different absorption spectra, we propose that CfbB converts Ni²⁺-hexahydrosirohydrochlorin *a,c*-diamide into a coenzyme F₄₃₀ variant lacking the lactam ring E and *seco*-F₄₃₀ into coenzyme F₄₃₀. Further activity assays with less CfbB showed that the conversion of *seco*-F₄₃₀ occurs much faster than that of Ni²⁺-hexahydrosirohydrochlorin *a,c*-diamide, establishing *seco*-F₄₃₀ as the true substrate for CfbB.

The structure of coenzyme F₄₃₀ formed by CfbB was confirmed by 2D heteronuclear NMR spectroscopy. It was not possible to obtain a complete dataset for coenzyme F₄₃₀ in D₂O as the ROESY and HMBC spectra were of poor quality. Therefore, we used the non-coordinating solvent 2,2,2-trifluoroethanol-*d*₃ (TFE-*d*₃), which allowed us to assign all resonances and thereby confirm the structure. Cyclization of the ring D propionate side chain was confirmed by the absence of a proton at the C10 position and the carbon chemical shift of C17 (ref. 32) observed at 200.34 p.p.m. The chemical shifts were in close agreement with previously published data³² (Extended Data Fig. 8, Supplementary Table 3). A mechanism for CfbB is shown in Extended Data Fig. 9.

Conclusion

The elucidation of the pathway for coenzyme F₄₃₀ biosynthesis (Fig. 5) completes our understanding of how the major members of the modified

process (*in vitro*), which might be enzyme-catalysed *in vivo*. The formal chemical changes for each step are given below the arrows not reflecting required cofactors or enzymatic mechanisms. The introduced structural changes are highlighted in red.

tetrapyrrole family are constructed. By using a rich tapestry of enzymes, it is possible to construct a broad range of complex small molecules, such as haem, chlorophyll, vitamin B₁₂ and coenzyme F₄₃₀, that are all derived from a common tetrapyrrole template and are involved in fundamental cellular processes, ranging from photosynthesis to respiration. Although the biosynthesis of molecules such as haem and chlorophyll has been understood for some time¹², recent research has led to the determination of the aerobic^{25,33} and anaerobic³⁴ pathways for vitamin B₁₂ biosynthesis, and the unexpected discovery of alternative routes for haem synthesis^{35,36}. By identifying the enzymes responsible for the transformation of sirohydrochlorin into coenzyme F₄₃₀, we have shown how the assembly of the molecular framework that is used to house nickel is orchestrated and optimised for its role in methanogenesis. Three of these biosynthetic steps require MgATP, reflecting the high energetic cost in making this specialized metallo-prosthetic group. Our understanding of F₄₃₀ synthesis will not only provide the opportunity to explore the development of recombinant methyl-coenzyme M reductase systems, a key component of which requires the synthesis of the essential F₄₃₀ coenzyme, but also lead to mechanistic studies of some very interesting enzymes.

Online Content Methods, along with any additional Extended Data display items and Source Data, are available in the online version of the paper; references unique to these sections appear only in the online paper.

Received 22 September 2016; accepted 25 January 2017.

Published online 22 February 2017.

- Ragsdale, S. W. Biochemistry of methyl-coenzyme M reductase: the nickel metalloenzyme that catalyzes the final step in synthesis and the first step in anaerobic oxidation of the greenhouse gas methane. *Met. Ions Life Sci.* **14**, 125–145 (2014).
- Thauer, R. K. Biochemistry of methanogenesis: a tribute to Marjory Stephenson. 1998 Marjory Stephenson Prize Lecture. *Microbiology* **144**, 2377–2406 (1998).
- Raghoebarsing, A. A. *et al.* A microbial consortium couples anaerobic methane oxidation to denitrification. *Nature* **440**, 918–921 (2006).
- Scheller, S., Goenrich, M., Boecher, R., Thauer, R. K. & Jaun, B. The key nickel enzyme of methanogenesis catalyses the anaerobic oxidation of methane. *Nature* **465**, 606–608 (2010).
- Shima, S. *et al.* Structure of a methyl-coenzyme M reductase from Black Sea mats that oxidize methane anaerobically. *Nature* **481**, 98–101 (2011).
- Krüger, M. *et al.* A conspicuous nickel protein in microbial mats that oxidize methane anaerobically. *Nature* **426**, 878–881 (2003).
- Ermler, U., Grabarse, W., Shima, S., Goubeaud, M. & Thauer, R. K. Crystal structure of methyl-coenzyme M reductase: the key enzyme of biological methane formation. *Science* **278**, 1457–1462 (1997).

8. Wongnate, T. & Ragsdale, S. W. The reaction mechanism of methyl-coenzyme M reductase: how an enzyme enforces strict binding order. *J. Biol. Chem.* **290**, 9322–9334 (2015).
9. Wongnate, T. *et al.* The radical mechanism of biological methane synthesis by methyl-coenzyme M reductase. *Science* **352**, 953–958 (2016).
10. Thauer, R. K. & Bonacker, L. G. Biosynthesis of coenzyme F₄₃₀, a nickel porphyrinoid involved in methanogenesis. *Ciba Found. Symp.* **180**, 210–222, discussion 222–227 (1994).
11. Gilles, H. & Thauer, R. K. Uroporphyrinogen III, an intermediate in the biosynthesis of the nickel-containing factor F₄₃₀ in *Methanobacterium thermoautotrophicum*. *Eur. J. Biochem.* **135**, 109–112 (1983).
12. Warren, M. J. & Scott, A. I. Tetrapyrrole assembly and modification into the ligands of biologically functional cofactors. *Trends Biochem. Sci.* **15**, 486–491 (1990).
13. Färber, G. *et al.* Coenzyme F₄₃₀ from methanogenic bacteria—complete assignment of configuration based on an X-ray-analysis of 12,13-diepi-F₄₃₀ pentamethyl ester and on NMR-spectroscopy. *Helv. Chim. Acta* **74**, 697–716 (1991).
14. Mucha, H., Keller, E., Weber, H., Lingens, F. & Trosch, W. Sirohydrochlorin, a precursor of factor-F₄₃₀ biosynthesis in *Methanobacterium thermoautotrophicum*. *FEBS Lett.* **190**, 169–171 (1985).
15. Pfaltz, A., Kobelt, A., Hüster, R. & Thauer, R. K. Biosynthesis of coenzyme F₄₃₀ in methanogenic bacteria. Identification of 15,17³-seco-F₄₃₀-17³-acid as an intermediate. *Eur. J. Biochem.* **170**, 459–467 (1987).
16. Brindley, A. A., Raux, E., Leech, H. K., Schubert, H. L. & Warren, M. J. A story of chelatase evolution: identification and characterization of a small 13–15-kDa “ancestral” cobaltochelate (CbiX^S) in the archaea. *J. Biol. Chem.* **278**, 22388–22395 (2003).
17. Yan, Y. *et al.* Crystal structure of *Escherichia coli* UDPMurNAc-tripeptide d-alanyl-d-alanine-adding enzyme (MurF) at 2.3 Å resolution. *J. Mol. Biol.* **304**, 435–445 (2000).
18. Staples, C. R. *et al.* Expression and association of group IV nitrogenase NifD and NifH homologs in the non-nitrogen-fixing archaeon *Methanocaldococcus jannaschii*. *J. Bacteriol.* **189**, 7392–7398 (2007).
19. Warren, M. J., Raux, E., Schubert, H. L. & Escalante-Semerena, J. C. The biosynthesis of adenosylcobalamin (vitamin B₁₂). *Nat. Prod. Rep.* **19**, 390–412 (2002).
20. Chivers, P. T. Nickel recognition by bacterial importer proteins. *Metallomics* **7**, 590–595 (2015).
21. Eitinger, T. & Mandrand-Berthelot, M. A. Nickel transport systems in microorganisms. *Arch. Microbiol.* **173**, 1–9 (2000).
22. Mulrooney, S. B. & Hausinger, R. P. Nickel uptake and utilization by microorganisms. *FEMS Microbiol. Rev.* **27**, 239–261 (2003).
23. Chivers, P. T., Benanti, E. L., Heil-Chapdelaine, V., Iwig, J. S. & Rowe, J. L. Identification of Ni-(L-His)₂ as a substrate for NikABCDE-dependent nickel uptake in *Escherichia coli*. *Metallomics* **4**, 1043–1050 (2012).
24. Waldron, K. J., Rutherford, J. C., Ford, D. & Robinson, N. J. Metalloproteins and metal sensing. *Nature* **460**, 823–830 (2009).
25. Deery, E. *et al.* An enzyme-trap approach allows isolation of intermediates in cobalamin biosynthesis. *Nat. Chem. Biol.* **8**, 933–940 (2012).
26. Bröcker, M. J. *et al.* Crystal structure of the nitrogenase-like dark operative protochlorophyllide oxidoreductase catalytic complex (ChIN/ChIB)₂. *J. Biol. Chem.* **285**, 27336–27345 (2010).
27. Muraki, N. *et al.* X-ray crystal structure of the light-independent protochlorophyllide reductase. *Nature* **465**, 110–114 (2010).
28. Fässler, A. *et al.* Preparation and properties of some hydrocorphinoid nickel(II)-complexes. *Helv. Chim. Acta* **65**, 812–827 (1982).
29. Schlingmann, G., Dresow, B., Ernst, L. & Koppenhagen, V. B. The structure of yellow metal-free and cobalt-containing corrinoids. *Liebigs Ann. Chem.* **2061–2066** (1981).
30. Schlingmann, G., Dresow, B., Koppenhagen, V. B., Becker, W. & Sheldrick, W. S. Structure of yellow metal-free and yellow cobalt-containing corrinoids. *Angew. Chem. Int. Edn Engl.* **19**, 321–322 (1980).
31. Lee, C. C., Ribbe, M. W. & Hu, Y. Cleaving the N,N triple bond: the transformation of dinitrogen to ammonia by nitrogenases. *Met. Ions Life Sci.* **14**, 147–176 (2014).
32. Won, H., Olson, K. D., Wolfe, R. S. & Summers, M. F. 2-dimensional NMR-studies of native coenzyme-F₄₃₀. *J. Am. Chem. Soc.* **112**, 2178–2184 (1990).
33. Battersby, A. R. How nature builds the pigments of life: the conquest of vitamin B₁₂. *Science* **264**, 1551–1557 (1994).
34. Moore, S. J. *et al.* Elucidation of the anaerobic pathway for the corrin component of cobalamin (vitamin B₁₂). *Proc. Natl Acad. Sci. USA* **110**, 14906–14911 (2013).
35. Bali, S. *et al.* Molecular hijacking of siroheme for the synthesis of heme and d₁ heme. *Proc. Natl Acad. Sci. USA* **108**, 18260–18265 (2011).
36. Dailey, H. A., Gerdes, S., Dailey, T. A., Burch, J. S. & Phillips, J. D. Noncanonical coproporphyrin-dependent bacterial heme biosynthesis pathway that does not use protoporphyrin. *Proc. Natl Acad. Sci. USA* **112**, 2210–2215 (2015).

Supplementary Information is available in the online version of the paper.

Acknowledgements We thank M. Höninger, T. Schnitzer and J. Streif for conducting initial experiments with CfbA and CfbC/CfbD. We thank R. Thauer and S. Shima for the gift of the F₄₃₀ standard. This work was supported by grants from the Boehringer Ingelheim Foundation (Exploration Grant) and the Deutsche Forschungsgemeinschaft (LA2412/6-1) to G.L. and from the Biotechnology and Biological Sciences Research Council (BBSRC; 68/B19356 and BB/I012079) to M.J.W.

Author Contributions S.J.M., S.T.S., C.S., E.D., A.D.L., J.V.R., S.B. and C.B. all undertook aspects of the experimental work, cloning, protein purification and enzyme assays, and helped with the interpretation of the data. P.T.C. provided the *nixA* clone and helped design the nickel uptake system. M.J.H., S.J.M. and A.D.L. designed and interpreted the NMR experiments and S.E.J.R., together with S.J.M. and A.D.L., provided the EPR data. S.J.M., M.J.W. and G.L. designed the experiments and wrote the paper.

Author Information Reprints and permissions information is available at www.nature.com/reprints. The authors declare no competing financial interests. Readers are welcome to comment on the online version of the paper. Correspondence and requests for materials should be addressed to M.J.W. (m.j.warren@kent.ac.uk) or G.L. (gunhild.layer@uni-leipzig.de).

METHODS

No statistical methods were used to predetermine sample size. The experiments were not randomized, and investigators were not blinded to allocation during experiments and outcome assessment.

Cloning of putative coenzyme F₄₃₀ biosynthetic genes. Genomic DNA of *Methanosarcina barkeri* strain Fusaro DSM804 was provided by R. Thauer. A list of the plasmids used in this work is given in Extended Data Table 1. Genes were PCR amplified using a forward primer containing NdeI or AseI and a reverse primer with both SpeI and BamHI restriction sites (see Extended Data Table 1). The SpeI site was added on the reverse primer for subsequent link and lock cloning³⁷. PCR fragments were digested with the relevant restriction enzymes and ligated into the pET14b plasmid. Genes were sequenced by GATC Biotech or Source BioScience LifeSciences. For the subcloning of Mbar_A0344 (*cfbA*), the gene was PCR amplified from pET14b-*cfbA* using primers *cbiX_AscI_fo* and *cbiX_SalI_re* (Extended Data Table 1). The resulting PCR fragment was digested with AseI and SalI and ligated into the correspondingly digested vector pETDuet-1 (Novagen/Merck Millipore). The *cfbA* gene Mbar_A0344 was then cut from this construct using the restriction enzymes NdeI and SalI, and the purified fragment was ligated into the correspondingly digested plasmid pET22b (Novagen), yielding expression plasmid pET22b-*cfbA* (Extended Data Table 1). For cloning of multi-gene constructs, sequenced genes were transferred into pET3a (to remove the His₆-tag), then constructed piecewise by the link-and-lock cloning method³⁷ in the pETCoco-2^{KAN} plasmid.

Recombinant protein production and purification of His₆-tagged proteins. *E. coli* Rosetta pLysS was transformed with plasmids containing putative coenzyme F₄₃₀ biosynthesis genes cloned into pET14b and selected on LB agar with 34 μg ml⁻¹ chloramphenicol and 100 μg ml⁻¹ ampicillin. For protein production, an overnight pre-culture was grown in LB medium for 16 h at 37 °C, 150 r.p.m. The next day, 10 ml of pre-culture was transferred into 1–4 l of LB medium with 34 μg ml⁻¹ chloramphenicol and 100 μg ml⁻¹ ampicillin. The cells were grown at 37 °C, 150 r.p.m. until an OD_{600 nm} of 1.0 was reached. Protein production was induced with 0.4 mM IPTG and cells were left overnight at 19 °C with 150 r.p.m. shaking. For increased production of iron-sulfur enzymes, 1 mM ammonium ferric citrate was added to the cultures at the induction stage. Proteins containing Fe-S clusters were purified in an anaerobic glovebox (Belle Technologies or Coy Laboratory Products), with O₂ levels at less than 2 p.p.m. All buffers and solutions were purged with argon before use in the glovebox. *E. coli* cultures were centrifuged at 5,180 g at 4 °C for 20 min. Cells were then resuspended in 15 ml of binding buffer (20 mM Tris-HCl, pH 8, 500 mM NaCl and 5 mM imidazole), followed by sonication under anaerobic conditions at 4 °C for 5 min with 10 and 30 s pulse and rest cycles, respectively. Cell lysates were centrifuged at 37,044 g at 4 °C for 20 min. The supernatant was then purified using 5 ml of pre-charged nickel chelated Sepharose. This was then washed with 50 ml of binding buffer, followed by washing steps (25 ml) containing increasing concentrations of imidazole from 30 to 70 mM. Elution was performed with buffer containing 400 mM imidazole. Purified protein was desalted on a pre-packed PD-10 column equilibrated in buffer without imidazole.

Recombinant production and purification of non-tagged CfbA. *E. coli* Rosetta pLysS containing plasmid pET22b-*cfbA* was cultivated as described above with the exception that the induction of protein production with IPTG was initiated when the cells had reached an OD_{600 nm} of about 0.4. After overnight cultivation the cells were collected by centrifugation and the cell pellet from 1 l of culture was resuspended in 20 ml of buffer A (50 mM Tris-HCl, pH 8) containing 1 mM phenylmethylsulfonyl fluoride (PMSF). Cells were disrupted by sonication and the resulting cell lysate was centrifuged in an ultracentrifuge at 175,000 g at 4 °C for 60 min. The soluble protein fraction was loaded onto a 1 ml HiTrap Q XL column (GE Healthcare) at a flow rate of 1 ml min⁻¹. The column was washed with 10 ml of buffer A and the bound proteins were then eluted using a linear NaCl gradient (0–400 mM NaCl in buffer A) developed over 20 ml. The CfbA-containing elution fractions were pooled, concentrated to 5 ml and then loaded onto a HiLoad 16/600 Superdex 75 prep grade column (GE Healthcare) equilibrated with 50 mM Tris-HCl, pH 8, 150 mM NaCl at a flow rate of 1 ml min⁻¹. The elution fractions containing CfbA were pooled and the buffer of the purified protein was exchanged inside the anaerobic chamber using a PD-10 column equilibrated with anaerobic test buffer (25 mM Tris-HCl, pH 8, 150 mM NaCl, 10 mM MgCl₂, 10% (v/v) glycerol). The purified CfbA was stored at –80 °C until further use.

Reconstitution of iron-sulfur clusters. The reconstitution of iron-sulfur clusters within CfbC and CfbD was performed as described previously³⁸. After reconstitution, the excess of iron and sulfide was removed by centrifugation and subsequent passage of the protein solution through a NAP-25 column (GE Healthcare), which was used according to the manufacturer's instructions. The iron and sulfide concentrations for Mbar_A0346 (CfbC) and Mbar_A0347 (CfbD) were determined as previously described³⁹. Protein concentration was estimated separately

using Bradford reagent (Bio-Rad Laboratories) with bovine serum albumin as a calibration standard.

EPR of CfbC and CfbD. Samples were prepared and then flash frozen in liquid nitrogen. EPR experiments were performed on a Bruker ELEXSYS E500 spectrometer operating at X-band, using a Super High Q cylindrical cavity (Q factor ≈ 16,000) equipped with an Oxford Instruments ESR900 liquid helium cryostat linked to an ITC503 temperature controller. Experimental parameters: microwave power 0.5 mW, field modulation amplitude 7 G, field modulation frequency 100 KHz, temperature 15 K.

Nickel chelatase activity assay (CfbA). Sirohydrochlorin was synthesized using the one-pot incubation method described previously⁴⁰. For the CfbA activity assay, 5 μM sirohydrochlorin and 50 μM of NiSO₄ were incubated at 37 °C with varying amounts of purified CfbA (0, 1, 1.5 and 2.5 μM) in anaerobic test buffer (50 mM Tris-HCl, pH 8, 150 mM NaCl, 10 mM MgCl₂ and 10% (v/v) glycerol) inside the anaerobic chamber. For each enzyme concentration the assay was performed at least three times. The deduced specific activity represents the mean value of all measurements. The chelation of nickel into sirohydrochlorin was monitored by recording UV/Vis absorption spectra at different time points using a V-650 spectrophotometer (Jasco).

Synthetic production of nickel-sirohydrochlorin *a,c*-diamide in *E. coli*. *E. coli* KRX auto-induction strain was transformed with the pETCoco-2^{KAN}-cobA-sirC-*cbiX*^S-*nixA* and pET14b-Mbar_A0348 plasmids using 0.2% (w/v) glucose to maintain the single copy state of the pETCoco-2^{KAN} derived plasmid and 25 μg ml⁻¹ kanamycin and 100 μg ml⁻¹ ampicillin for antibiotic selection. An overnight pre-culture was grown for 16 h at 28 °C, 150 r.p.m. The next day 10 ml of pre-culture was transferred into 1 l of 2YT medium with 50 μg ml⁻¹ kanamycin, 100 μg ml⁻¹ ampicillin, 0.05% glucose (w/v), 0.1% rhamnose (w/v), 0.01% (w/v) arabinose and between 25 μM and 100 μM NiCl₂·6H₂O. The cells were grown at 28 °C and 150 r.p.m. for 24 h. This yields approximately 1–2 mg l⁻¹ of nickel-sirohydrochlorin *a,c*-diamide in complex with the His₆-tagged amidotransferase Mbar_A0348 (CfbE) enzyme, which can be purified using IMAC purification under low-salt (100 mM) buffer conditions.

Amidotransferase kinetics (CfbE). The protocol for the antimony-phosphomolybdate colorimetric based stopped-assay⁴¹ was used for determining the ATPase activity of the *M. barkeri* CfbE amidotransferase in the presence of its substrate nickel-sirohydrochlorin. 0.2% (w/v) citric acid was added after a time delay of 2 min to prevent background increases in absorbance from acid hydrolysis of ATP. Assays were performed in buffer B (20 mM Tris-HCl, pH 8 and 100 mM NaCl buffer) at 20 °C.

Amide ¹⁵N labelling ATP titration experiment and NMR of nickel-sirohydrochlorin *a,c*-diamide. (¹⁵NH₃)₂SO₄ (Cambridge Isotope Laboratories) was used for labelling of the amide side chains. Single-turnover reactions were prepared in 10 ml of buffer B with 25 μM of pure *M. barkeri* CfbE, 25 μM nickel-sirohydrochlorin, 1 mM MgCl₂, 25 mM (¹⁵NH₃)₂SO₄. Turnover was controlled by an ATP titration series of 0, 25, 50 and 100 μM. Reactions were left for 30 min at 37 °C. The reaction product was purified, dehydrated and dissolved in d₆-DMSO in order to reduce proton solvent exchange to allow observation of the NH amide signals, which are barely detectable in D₂O or acidic (pH 5) 1:10 H₂O/D₂O mixtures. Two-dimensional datasets were collected including ¹H-¹⁵N HSQC, ¹H-¹H NOESY and ¹H-¹⁵N HSQC-TOCSY spectra. The ¹H-¹⁵N correlation spectra were collected by the SOFAST-HSQC method, which increases sensitivity using fast repetition rates⁴². This method resolved four clear amide peaks with no background signals (Extended Data Fig. 2). These were correlated to show clear NOE through space interactions with the ring A and C propionate side chains as indicated in the ROESY and NOESY spectra (Extended Data Fig. 3; Supplementary Table 1). This provides strong evidence for the positioning of the amide groups at the *a* and *c* positions, thus confirming the product of the CfbE amidation reaction as Ni²⁺-sirohydrochlorin *a,c*-diamide.

LC-MS of nickel-sirohydrochlorin and nickel-sirohydrochlorin *a,c*-diamide. Samples (10–100 μl) were injected onto an Ace 5 AQ column (2.1 × 150 mm, 5 μm, Advanced Chromatography Technologies) that was attached to an Agilent 1100 series HPLC coupled to a microTOF-Q (Bruker) mass spectrometer and equipped with online diode array and fluorescence detectors and run at a flow rate of 0.2 ml min⁻¹. Tetrapyrroles were routinely separated with a linear gradient of acetonitrile in 0.1% TFA. Mass spectra were obtained using an Agilent 1100 liquid chromatography system connected to a Bruker micrOTOF II MS, using electrospray ionisation in positive mode. UV/Vis absorption spectra were monitored by DAD-UV detection (Agilent Technologies).

Nickel-sirohydrochlorin *a,c*-diamide reductase activity assay (CfbC/CfbD). The assay for testing the reductase activity of CfbC/CfbD was performed under anaerobic conditions at 37 °C in anaerobic test buffer (50 mM Tris-HCl, pH 8, 150 mM NaCl, 10 mM MgCl₂ and 10% (v/v) glycerol). The assay contained

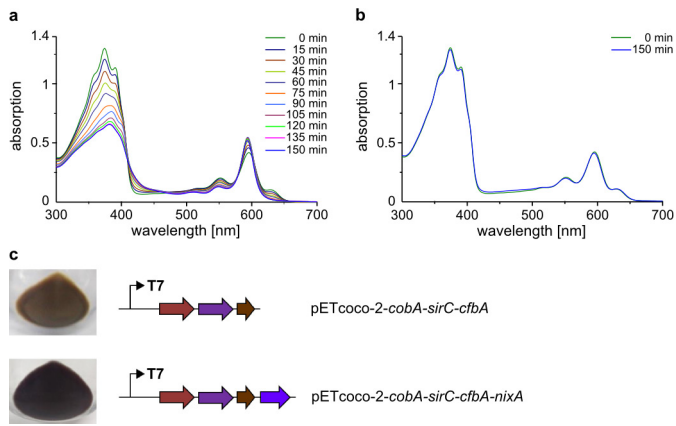
10 μ M nickel-sirohydrochlorin *a,c*-diamide (formed *in situ* by the action of CfbE), 10 μ M CfbC, 10 μ M CfbD, 3.2 mM ATP, 3.2 mM sodium dithionite and residual amounts of the enzymes HemB, HemC, HemD, CobA, SirC, CfbA and CfbE, which were used for the formation of nickel-sirohydrochlorin *a,c*-diamide. The reaction was followed by UV/Vis absorption spectroscopy and by analysing the tetrapyrrole content of the assay mixtures after 0, 1.5, 14 and 22 h of incubation by HPLC. For HPLC analysis, the tetrapyrroles were extracted by denaturation of the proteins using guanidinium chloride. For this, 160 mg of guanidinium chloride were dissolved in 300 μ l of the sample, and the mixture was incubated for 2 min at room temperature. Subsequently, the free tetrapyrroles were separated from the denatured proteins by ultrafiltration using an Amicon Ultra 10k filter unit (Merck Millipore). The tetrapyrrole-containing filtrate (40 μ l injection volume) was analysed by HPLC using a ReproSil-Pur C18 AQ column (Dr. Maisch HPLC GmbH) and a JASCO HPLC 2000 series system (Jasco). The separation was carried out at a flow rate of 0.2 ml min⁻¹. Solvent A was 0.01% formic acid in H₂O and solvent B was acetonitrile. Tetrapyrroles eluted with a linear gradient system within 25 min: start conditions 95% A/5% B and end conditions 65% A/35% B. The tetrapyrroles were detected by photometric diode array analysis in the range of 220–670 nm. The masses of the eluting tetrapyrroles were confirmed by ESI-MS analysis on an Esquire 3000+ ESI ion trap mass spectrometer coupled to an Agilent 1100er series HPLC system using the same column, eluent, and gradient. Scan was carried out in alternating mode between *m/z* 500–2000, the target mass set to *m/z* 1,000, nebulizer pressure to 70 p.s.i., dry gas flow to 11 l min⁻¹ and dry gas temperature to 360 °C.

Ring F ligase activity assay (CfbB). The CfbB assay was conducted under anaerobic conditions at 37 °C in anaerobic test buffer (50 mM Tris-HCl, pH 8, 150 mM NaCl, 10 mM MgCl₂, 10% (v/v) glycerol). The assay contained 7.5 μ M of either Ni²⁺-hexahydrochlorin *a,c*-diamide or *seco*-F₄₃₀ (formed as described for the CfbC/CfbD assay), 0.75 μ M or 7.5 μ M CfbB and 3.2 mM ATP. After 1 or 2 h of incubation, the tetrapyrroles were extracted and analysed by HPLC and HPLC-MS as described for the CfbC/CfbD assay.

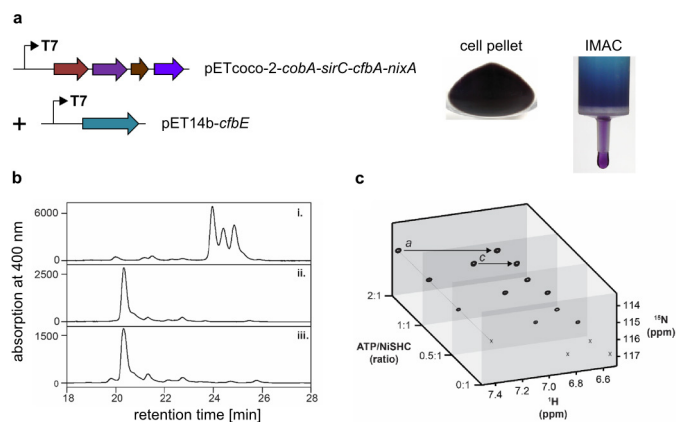
NMR of *seco*-F₄₃₀. For structural determination an isotopically enriched sample (4 mM) of the *seco*-F₄₃₀ intermediate was prepared using ¹⁵N-glutamine as the amide donor and the incorporation of two ¹⁵N atoms in the product was confirmed by HPLC-MS. Analysis of the data following assignment established the presence of the lactam attached to ring B. This was determined from the combination of the following pieces of information. Protons attached to C3-C4-C5 are present in a single scalar coupled network and C5 (36.37 p.p.m.) appears sp³ hybridized with two germinal protons (1.56 and 1.84 p.p.m.). The chemical shift of C6, assigned from the ¹H-¹³C HMBC spectrum, is 96.39 p.p.m.. Lastly, the ¹⁵N HSQC clearly shows 3 signals from which the germinal pair of protons was assigned to the NH₂ of the *a*-sidechain (N23) and the single N-H resonance observed at lower field to the lactam formed from the *c*-sidechain of ring B (N73) (Extended Data Fig. 6).

Data availability. All data generated or analysed during this study are available within the paper (and its Supplementary Information files).

37. McGoldrick, H. M. *et al.* Identification and characterization of a novel vitamin B₁₂ (cobalamin) biosynthetic enzyme (CobZ) from *Rhodobacter capsulatus*, containing flavin, heme, and Fe-S cofactors. *J. Biol. Chem.* **280**, 1086–1094 (2005).
38. Flühe, L. *et al.* The radical SAM enzyme AlbA catalyzes thioether bond formation in subtilisin A. *Nat. Chem. Biol.* **8**, 350–357 (2012).
39. Kühner, M. *et al.* The alternative route to heme in the methanogenic archaeon *Methanosarcina barkeri*. *Archaea* **2014**, 327637 (2014).
40. Schubert, H. L. *et al.* The structure of *Saccharomyces cerevisiae* Met8p, a bifunctional dehydrogenase and ferrochelatase. *EMBO J.* **21**, 2068–2075 (2002).
41. Bartolommei, G., Moncelli, M. R. & Tadini-Buoninsegni, F. A method to measure hydrolytic activity of adenosinetriphosphatases (ATPases). *PLoS One* **8**, e58615 (2013).
42. Schanda, P., Kupce, E. & Brutscher, B. SOFAST-HMQC experiments for recording two-dimensional heteronuclear correlation spectra of proteins within a few seconds. *J. Biomol. NMR* **33**, 199–211 (2005).



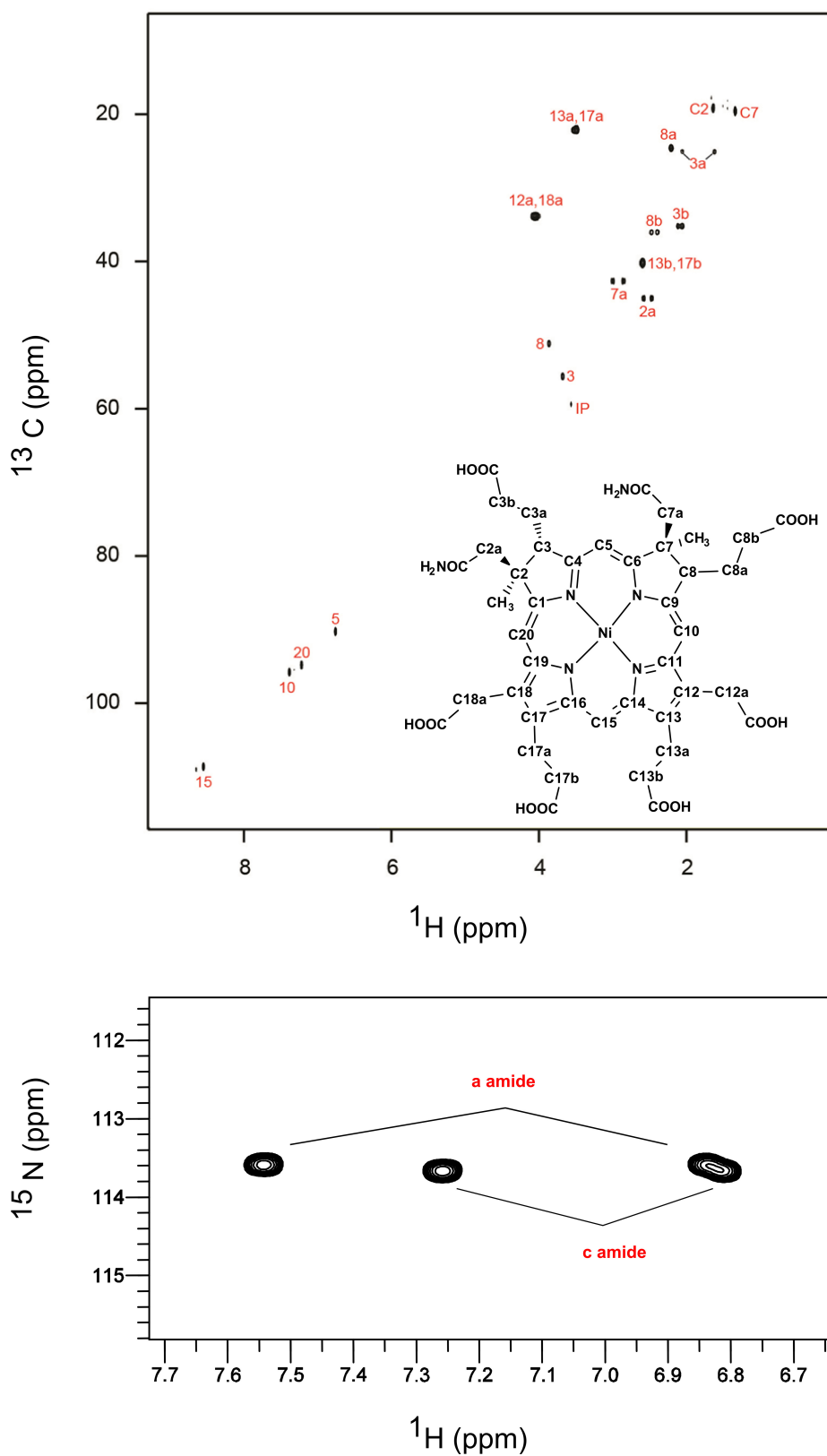
Extended Data Figure 1 | Nickel chelatase activity of CfbA. a, b, *In vitro* activity assay of CfbA. Purified CfbA was incubated with sirohydrochlorin and NiSO_4 at 37 °C (a). The insertion of nickel was monitored by UV/Vis absorption spectroscopy every 15 min. When CfbA was omitted from the assay mixture (b), no nickel insertion was observed. c, *In vivo* activity of CfbA. Cell pellets of *E. coli* cells transformed with either pETcoco-2-cobA-sirC-cfbA or pETcoco-2-cobA-sirC-cfbA-nixA grown in the presence of nickel.



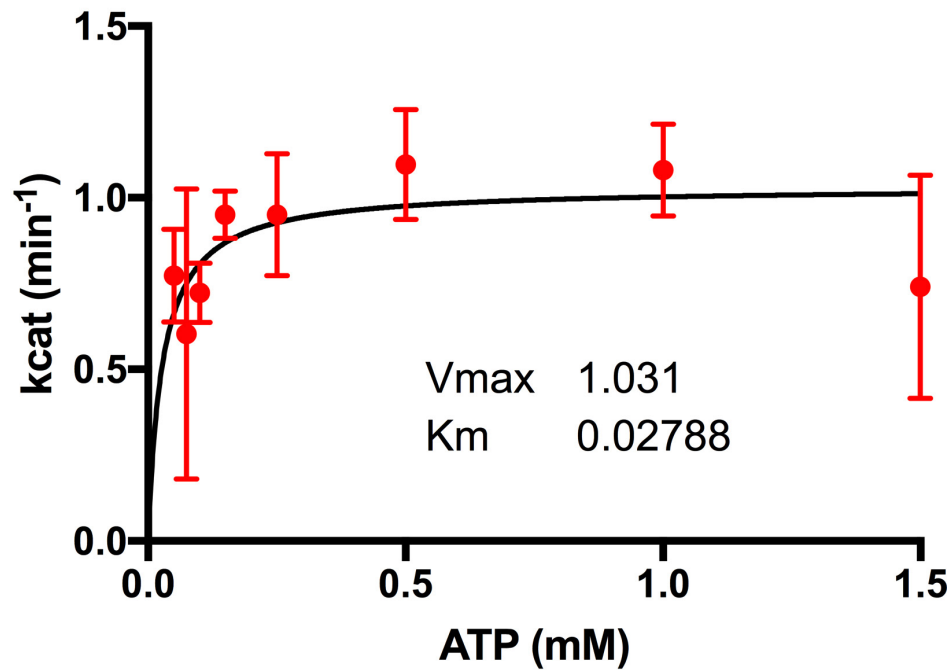
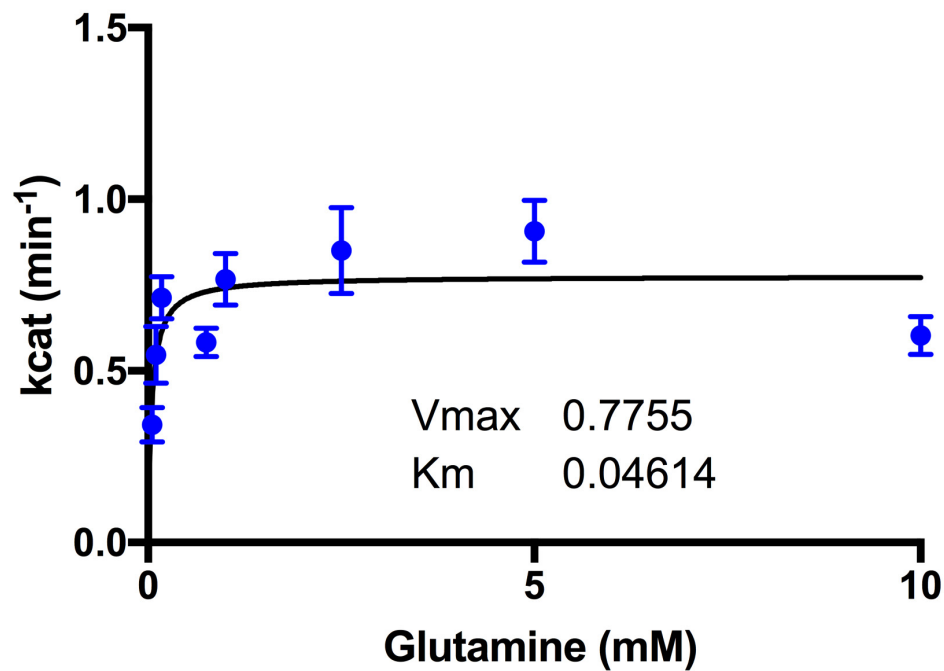
Extended Data Figure 2 | Amidotransferase activity of CfbE.

a, *In vivo* activity of CfbE. *E. coli* cells transformed with pETcoco-2-cobA-sirC-cfbA-nixA and pET14b-cfbE and grown in the presence of nickel produce a dark violet pigment that co-purifies with CfbE during IMAC.

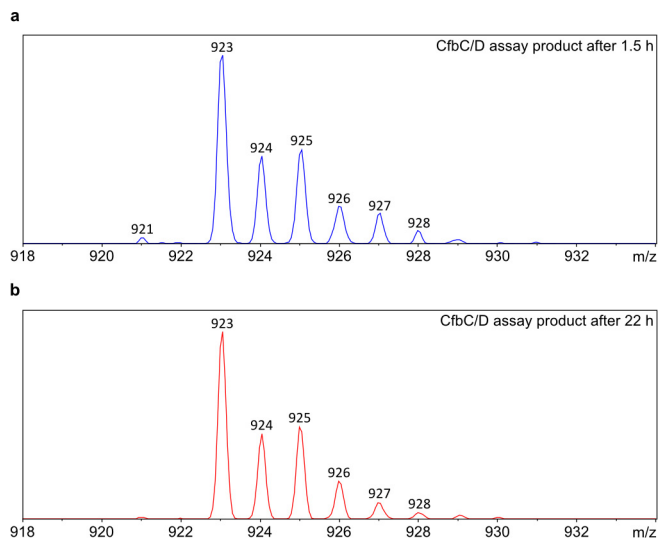
b, **c**, ^{15}N labelling of nickel-sirohydrochlorin a,c -diamide. **b**, Reverse-phase HPLC chromatogram of nickel-sirohydrochlorin substrate, $m/z = 919$ (i); unlabelled nickel-sirohydrochlorin a,c -diamide, $m/z = 917$ (ii); and ^{15}N labelled nickel-sirohydrochlorin a,c -diamide, $m/z = 919$ (iii). **c**, ^1H - ^{15}N HSQC of an ATP limited titration with nickel-sirohydrochlorin, CfbE and $^{15}\text{NH}_3$. The *a* and *c* amide groups increase proportionally in intensity as the level of ATP increases.



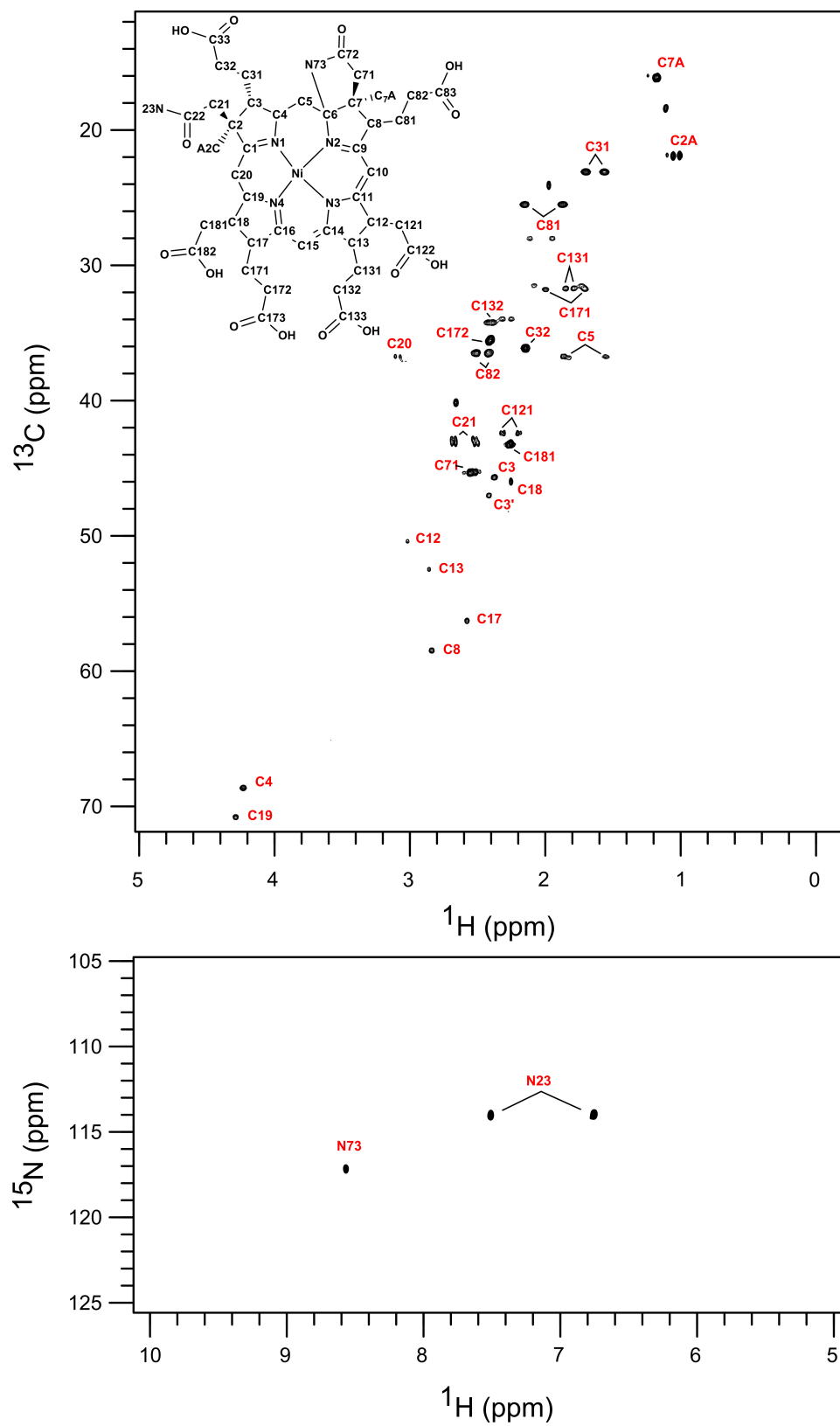
Extended Data Figure 3 | NMR characterization of Ni^{2+} -sirohydrochlorin *a,c*-diamide. a, b, ^1H - ^{13}C HSQC (a) and ^1H - ^{15}N HSQC (b) of 4 mM Ni^{2+} -sirohydrochlorin *a,c*-diamide in D_2O .

A**B**

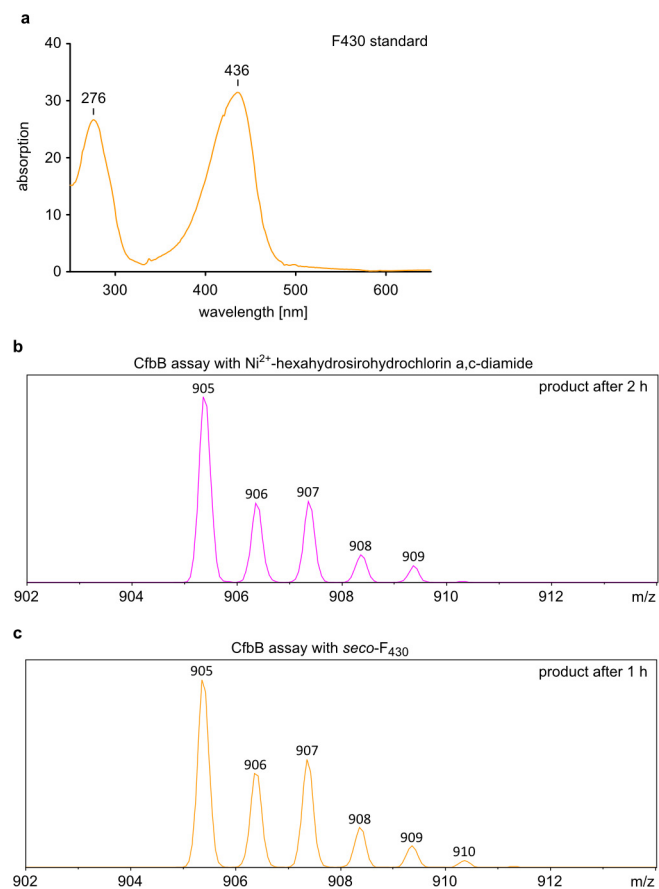
Extended Data Figure 4 | Steady-state kinetics of the *M. barkeri* CfbE amidotransferase with glutamine or ATP as a variable. a, 1 mM glutamine with ATP varied between 0.05 and 1.5 mM ATP. b, 0.5 mM ATP with glutamine varied between 0.05 and 10 mM. Fixed conditions: buffer B, 20 °C, 2.5 μM *M. barkeri* CfbE, 25 μM nickel-sirohydrochlorin, 5 mM MgCl_2 . The mean and error bars were calculated from 3 technical repeats.



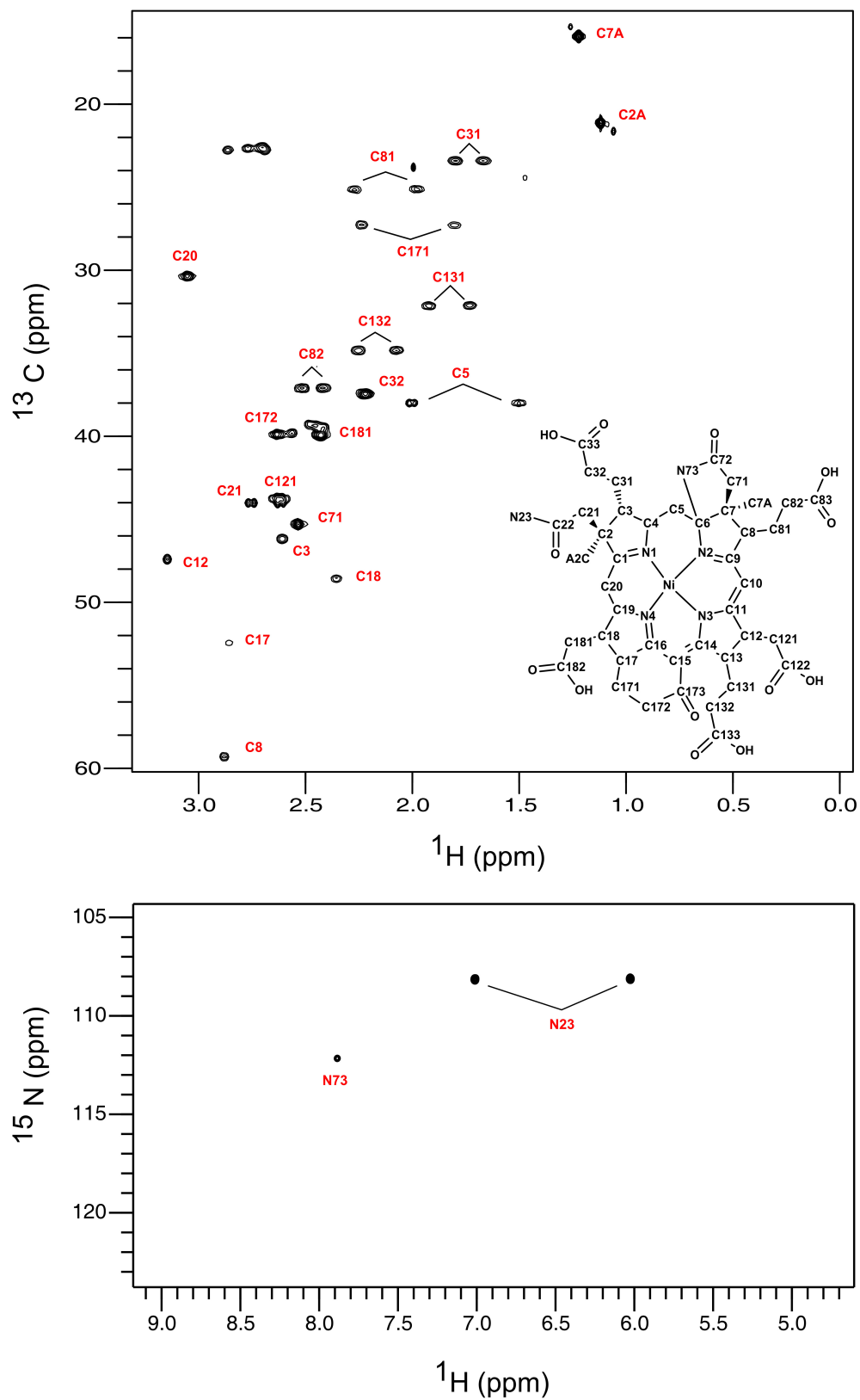
Extended Data Figure 5 | Characterization of the CfbC/CfbD assay reaction products by mass spectrometry after HPLC separation. a, Mass spectrum with the isotopic pattern of the reaction product after 1.5 h of incubation measured in positive ion mode. **b,** Mass spectrum with the isotopic pattern of the reaction product after 22 h of incubation measured in positive ion mode.



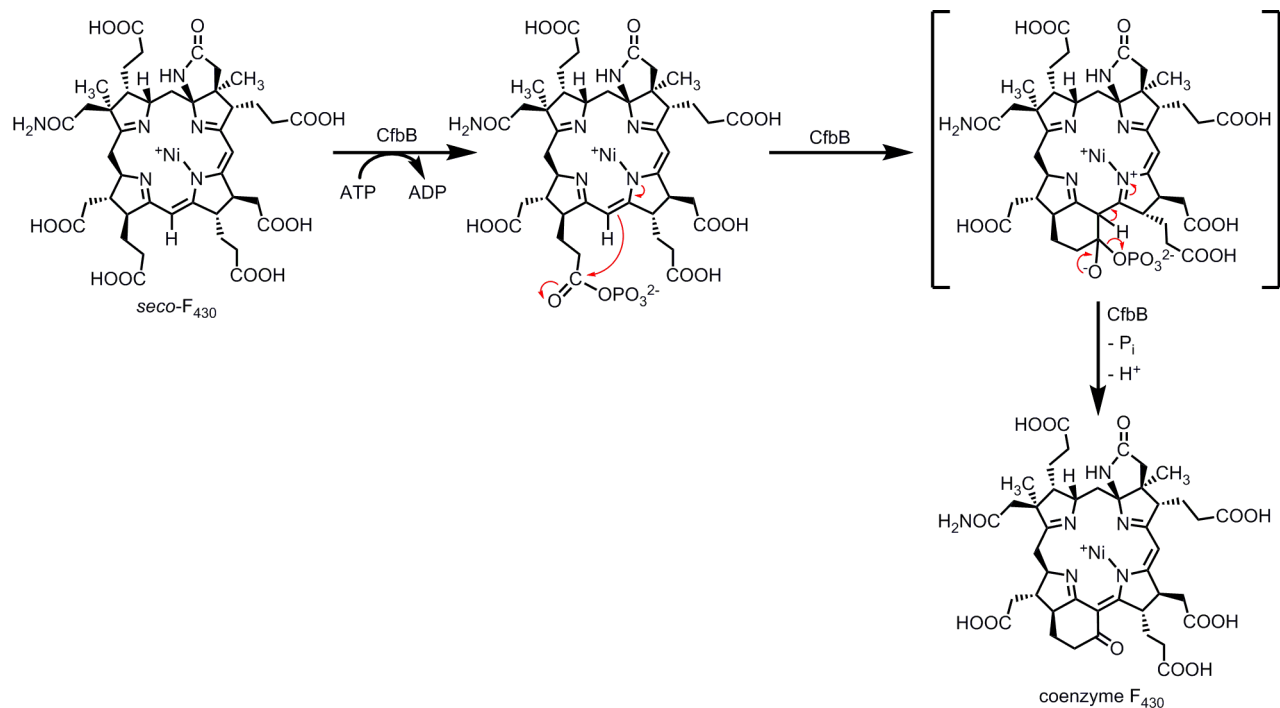
Extended Data Figure 6 | NMR characterization of *seco*-F₄₃₀. a, b, ¹H-¹³C HSQC (a) and ¹H-¹⁵N HSQC (b) of 4 mM *seco*-F₄₃₀ in D₂O.



Extended Data Figure 7 | Characterization of the CfbB assay reaction products. **a**, UV/Vis absorption spectrum of an F₄₃₀ standard in 0.01% formic acid/acetonitrile. **b**, CfbB assay with Ni²⁺-hexahydrochlorin *a,c*-diamide as the substrate. Mass spectrum with the isotopic pattern of the reaction product after 2 h of incubation measured in positive ion mode after HPLC separation. **c**, CfbB assay with *seco*-F₄₃₀ as the substrate. Mass spectrum with the isotopic pattern of the reaction product after 22 h of incubation measured in positive ion mode after HPLC separation.



Extended Data Figure 8 | NMR characterization of F₄₃₀ synthesized by CfbB. ¹H-¹³C HSQC and ¹H-¹⁵N HSQC of F₄₃₀ in TFE-*d*₃.



Extended Data Figure 9 | Proposed mechanism for the reaction catalysed by CfbB. Initially, CfbB promotes the ATP-dependent phosphorylation of the propionic acid side chain on ring D of *seco*-F₄₃₀. This activated side chain is then able to undergo cyclisation to form ring F and thereby generate coenzyme F₄₃₀.

Extended Data Table 1 | Plasmids and primers used in this study

Plasmid		Source
pMH003 – Iron sulfur cluster (<i>isc</i>) biogenesis operon from <i>E. coli</i>		(7)
pET22b- <i>nixA</i> – Nickel transporter from <i>H. pylori</i>		This work
pETcoco-2 ^{KAN}		(8)
pETcoco-2 ^{KAN} - <i>cobA</i>		This work
pETcoco-2 ^{KAN} - <i>cobA-sirC</i>		This work
pETcoco-2 ^{KAN} - <i>cobA-sirC-cfbA</i>		This work
pETcoco-2 ^{KAN} - <i>cobA-sirC-cfbA-nixA</i>		This work
pET14b- <i>cfbA</i> (Mbar_A0344)		This work
pET14b- <i>cfbB</i> (Mbar_A0345)		This work
pET14b- <i>cfbC</i> (Mbar_A0346)		This work
pET14b- <i>cfbD</i> (Mbar_A0347)		This work
pET14b- <i>cfbE</i> (Mbar_A0348)		This work
pET14b- <i>cfbC-cfbD-isc</i>		This work
pET14b- <i>cfbD-cfbC-isc</i>		This work
pET22b- <i>cfbA</i>		This work
pET3a- <i>cobA</i>		This work
pET3a- <i>sirC</i>		This work
pET3a- <i>cfbA</i> (Mbar_A0344)		This work
pET3a- <i>nixA</i>		This work
Primer	Sequence	Site
MB0344 F	CACCATATGACAGAAAACTCG	NdeI
MB0344 R	GTGGGATCCACTAGTTAAAGGGCTTCCTGAACC	BamHI/SpeI
MB0345 F	CACCATATGGACCTGTACCGGAAG	NdeI
MB0345 R	GTGGGATCCACTAGTTAACGGAAGCATTTTACC	BamHI/SpeI
MB0346 F	CACCATATGGCTGAAAAAGAGATTTTC	NdeI
MB0346 R	GTGGGATCCACTAGTCAGGCTTCCTTTGCAAC	BamHI/SpeI
MB0347 F	CACATGAAAAACCAGAAGATC	NdeI
MB0347 R	GTGGGATCCACTAGTTATTTTGTTAATTCC	BamHI/SpeI
MB0348 F	CGCCATATGCTTAACGACAAGCAATCC	NdeI
MB0348 R	ATGGGATCCACTAGTTCACGGAAGAACCCTGG	BamHI/SpeI
<i>cbiX_AscI_fo</i>	TATAGGCGCGCCAAGAAGGAGATATACC	AscI
<i>cbiX_SalI_re</i>	TATAGTCGACTTAAAGGGCTTCCTGAACC	SalI

Author Queries

Journal: **Nature**Paper: **nature21427**Title: **Elucidation of the biosynthesis of the methane catalyst coenzyme F₄₃₀**

Query Reference	Query
1	<p>AUTHOR: When you receive the PDF proof, please check that the display items are as follows (doi:10.1038/nature21427): Figs 1–5 (colour); Tables: None; Boxes: None; Extended Data display items: Figs: 1–9; Tables: 1</p> <p>Please check the edits to all main-text figures very carefully, and ensure that any error bars in the figures are defined in the figure legends. If you wish to revise the Extended Data items for consistency with main-text figures and tables, please copy the style shown in the PDF proof (such as italicising variables and gene symbols, and using initial capitals for labels) and return the revised Extended Data items to us along with your proof corrections.</p>
2	AUTHOR: Sentence change (with respect to DPOR) OK? 
Web summary	The enzymes and pathway involved in the biosynthesis of coenzyme F ₄₃₀ are identified, completing our understanding of how members of the cyclic modified tetrapyrrole family are constructed.

For Nature office use only:

Layout	<input type="checkbox"/>	Figures/Tables/Boxes	<input type="checkbox"/>	References	<input type="checkbox"/>
DOI	<input type="checkbox"/>	Error bars	<input type="checkbox"/>	Supp info	<input type="checkbox"/>
Title	<input type="checkbox"/>	Colour	<input type="checkbox"/>	Acknowledgements	<input type="checkbox"/>
Authors	<input type="checkbox"/>	Text	<input type="checkbox"/>	Author contribs	<input type="checkbox"/>
Addresses	<input type="checkbox"/>	Methods	<input type="checkbox"/>	COI	<input type="checkbox"/>
First para	<input type="checkbox"/>	Received/Accepted	<input type="checkbox"/>	Correspondence	<input type="checkbox"/>
		AOP	<input type="checkbox"/>	Author corr	<input type="checkbox"/>
		Extended Data	<input type="checkbox"/>	Web summary	<input type="checkbox"/>
				Accession codes link	<input type="checkbox"/>
				Referee accreditation	<input type="checkbox"/>

SUBJECT WORDS

Biological sciences/Biochemistry/Enzymes [URI /631/45/607]; Biological sciences/Chemical biology/Biosynthesis [URI /631/92/60].

TECHNIQUE TERMS

Techniques: Life sciences techniques, Protein techniques [Protein purification]; Life sciences techniques, Protein techniques [Protein expression]; Life sciences techniques, Protein techniques [Mass spectrometry]; Physical sciences techniques, Spectroscopy [NMR spectroscopy]; Life sciences techniques, Genomic analysis [PCR-based techniques].